

Spectrum of $4d \mathcal{N} = 1$ SYM on the lattice with light dynamical Wilson gluinos

K. Demmouche, F. Farchioni*, A. Ferling, G. Münster, J. Wuilloud

*University of Münster, Institute for Theoretical Physics
Wilhelm-Klemm-Strasse 9, D-48149 Münster, Germany
E-mail: k_demm01@uni-muenster.de, farchion@uni-muenster.de*

I. Montvay

Deutsches Elektronen-Synchrotron DESY, Notkestr. 85, D-22603 Hamburg, Germany

E.E. Scholz

Physics Department, Brookhaven National Laboratory, Upton, NY 11973, USA

We perform Monte Carlo investigations of the $4d \mathcal{N} = 1$ supersymmetric Yang-Mills (SYM) theory on the lattice with dynamical gluinos in the adjoint representation of the $SU(2)$ gauge group. Our aim is to determine the mass spectrum of the low-lying bound states which is expected to be organised in supermultiplets in the infinite volume continuum limit. For this purpose we perform simulations on large lattices, up to an extension $L/r_0 \simeq 6$ where $r_0 \simeq 0.5 \text{ fm}$ is the Sommer scale parameter. We apply improved lattice actions: tree-level improved Symanzik (tlSym) gauge action and in the later runs a Stout-smearred Wilson fermion action. The gauge configuration samples are prepared by the Two-Step Polynomial Hybrid Monte Carlo (TS-PHMC) update algorithm.

*The XXVI International Symposium on Lattice Field Theory
July 14 - 19, 2008
Williamsburg, Virginia, USA*

*Speaker.

1. Introduction

The $\mathcal{N} = 1$ supersymmetric Yang-Mills (SYM) theory is the minimal SUSY extension of the $SU(N_c)$ Yang-Mills theory. The fermionic degrees of freedom, the *gluinos*, are given by the superpartners of the gauge fields A_μ^a (*gluons*) and are described by Majorana spinors λ_a ($a = 1 \dots N_c^2 - 1$) transforming according to the adjoint representation of the gauge group. SYM is characterized by a rich low-energy dynamics with interesting aspects as confinement and spontaneous breaking of a discrete chiral symmetry – a continuum $U(1)$ chiral symmetry is missing at the quantum level due to the Adler-Bell-Jackiw anomaly. SYM can be related to QCD with a single quark flavour ($N_f = 1$ QCD), where the Majorana spinor is replaced by the single Dirac spinor. The latter model is also object of investigation by our collaboration [1].

This work represents a continuation of a long-standing project of the DESY-Münster-Roma Collaboration (DMRC) for the simulation of $SU(2)$ SYM, see [2] for a review and [3] for more recent results. Following [4] we apply the Wilson approach, which has been proved to be successful in lattice QCD computations in spite of its known limitations. SUSY is broken by the lattice discretisation and, in the Wilson approach, by the Wilson term. It is expected to be recovered in the continuum limit by properly tuning the only relevant parameter, the bare gluino mass, to a critical value corresponding to massless gluinos. Another (related) inconvenience of the Wilson discretisation, namely a non positive-definite fermion measure even for positive gluino masses, turns out to have no appreciable impact in practical applications.

Past simulations of DMRC were performed on quite fine lattices,¹ $a \simeq 0.08$ fm, but in a small volume, $L \simeq 1$ fm; this setup was appropriate for the study of the SUSY Ward identities [5], also valid in a finite volume. We now concentrate on the mass spectrum of bound states for which low-energy effective theories predict a reorganisation of the masses in two supermultiplets at the SUSY point [6, 7]. Thanks to a new more efficient simulation algorithm (see below) and enhanced computing resources we are now able to accumulate relevant statistics on larger lattices. Our present series of numerical simulations are performed on $16^3 \cdot 32$ and $24^3 \cdot 48$ lattices with lattice spacing $a \simeq 0.125$ fm. The lattice extension $L \simeq 2 - 3$ fm is expected to be large enough to allow control over finite volume effects on the bound states masses. Simulations on finer lattices are planned.

2. Lattice formulation and algorithms

2.1 Lattice formulation

We apply the tree-level Symanzik (tlSym) improved gauge action for the gauge part including rectangular Wilson loops of perimeter six:

$$S_g = \beta \left(c_0 \sum_{pl} \left\{ 1 - \frac{1}{N_c} \text{ReTr} U_{pl} \right\} + c_1 \sum_{rec} \left\{ 1 - \frac{1}{N_c} \text{ReTr} U_{rec} \right\} \right), \quad (2.1)$$

with $c_0 = 1 - 8c_1$ and $c_1 = -1/12$ in the case of tlSym action.

The contribution of the gluino to the effective gauge action is given by

$$S_{\tilde{g}}^{eff} = -\frac{1}{2} \log \det Q[U], \quad (2.2)$$

¹We use QCD units for setting the scale. The Sommer scale parameter is fixed to the value $r_0 \equiv 0.5$ fm.

where Q is the non-hermitian Dirac-Wilson fermion matrix defined by

$$Q_{xy}^{ab}[U] = \delta_{xy} \delta^{ab} - \kappa \sum_{\mu=1}^4 (\delta_{x,y+\hat{\mu}} (1 + \gamma_{\mu}) V_{\mu}^{ab}(y) + \delta_{x+\hat{\mu},y} (1 - \gamma_{\mu}) V_{\mu}^{Tab}(x)); \quad (2.3)$$

$V_{\mu}(x)$ is the adjoint gauge link, a real orthogonal matrix:

$$V_{\mu}^{ab}[U](x) = 2\text{Tr}\{U_{\mu}^{\dagger}(x) T^a U_{\mu}(x) T^b\} = V_{\mu}^{*ab}(x) = [V_{\mu}^{-1ab}(x)]^T. \quad (2.4)$$

(T^a are the generators of the $SU(N_c)$ group. In case of $SU(2)$ one has $T^a = \frac{1}{2} \sigma^a$ with the Pauli matrices σ^a .) Observe that $\det Q \geq 0$ for Majorana fermions. In our recent simulations the links $U_{x,\mu}$ in the Wilson-Dirac operator Eq. (2.3) are replaced by stout-smear links [8], which are defined as

$$U_{x,\mu}^{(1)} \equiv U_{x,\mu} \exp \left\{ \frac{1}{2} (\Omega_{x,\mu} - \Omega_{x,\mu}^{\dagger}) - \frac{1}{4} \text{Tr} (\Omega_{x,\mu} - \Omega_{x,\mu}^{\dagger}) \right\}, \quad \Omega_{x,\mu} \equiv U_{x,\mu}^{\dagger} C_{x,\mu} \quad (2.5)$$

where $C_{x,\mu}$ is a sum over staples

$$C_{x,\mu} \equiv \sum_{v \neq \mu} \rho_{\mu v} \left(U_{x+\hat{\mu},v}^{\dagger} U_{x+\hat{v},\mu} U_{x,v} + U_{x-\hat{v}+\hat{\mu},v} U_{x-\hat{v},\mu} U_{x-\hat{v},v}^{\dagger} \right). \quad (2.6)$$

We apply one step of smearing with smearing parameters $\rho_{\mu v} = 0.15$ in all lattice directions.

2.2 Updating algorithm

The factor in front of $\log \det(Q)$ in the Curci-Veneziano action reproduces the absolute value of the Pfaffian for Majorana fermions. Effectively, it corresponds to a flavour number $N_f = \frac{1}{2}$. The sign of the Pfaffian can be included in a reweighting procedure (see below). In our numerical simulations we use the two-step polynomial hybrid Monte Carlo (TS-PHMC) algorithm [9] which is based on a two-step polynomial approximation [10]. The fermion determinant is represented as

$$\det(Q)^{N_f} = \{\det(Q^{\dagger} Q)\}^{N_f/2} \simeq \frac{1}{\det P_{n_1}(Q^{\dagger} Q) P_{n_2}(Q^{\dagger} Q)} \quad (2.7)$$

with the condition on the polynomials P_n

$$\lim_{n_2 \rightarrow \infty} P_{n_1}(x) P_{n_2}(x) = x^{-N_f/2}, \quad x \in [\varepsilon, \lambda], \quad (2.8)$$

where the interval covers the spectrum of $Q^{\dagger} Q$. The order of the first polynomial n_1 is chosen as low as possible provided that the acceptance in the accept-reject step done with P_{n_2} , after a sequence of PHMC trajectories prepared with P_{n_1} , is sufficiently high (in our cases 80-90%).

In earlier simulations of the DESY-Münster collaboration the two-step multi boson (TSMB) algorithm [10] was used for the SYM theory. There the updating is performed by heatbath and overrelaxation sweeps for the pseudofermions and Metropolis and heatbath sweeps for gauge field. In case of the TS-PHMC algorithm, which is more effective in producing short autocorrelations among the gauge configurations, PHMC trajectories are created by applying the Sexton-Weingarten integration scheme with multiple time scales and, as usual, Metropolis accept-reject at the end of each trajectory. After the update sweeps/trajectories the second high-precision polynomial P_{n_2} is

used in a stochastic *noisy correction step* with a global accept-reject condition. The polynomial P_{n_2} , which is an approximation for $[x^{-N_f/2}P_{n_1}]^{-1}$, has to be highly precise so that the error of the approximation is negligible compared to the overall statistical error, provided that the spectrum of $Q^\dagger Q$ is in the interval $[\varepsilon, \lambda]$.

If some of the eigenvalues is outside $[\varepsilon, \lambda]$ then the approximations are not precise enough and a reweighting procedure has to be applied by an appropriately chosen high order polynomial. This gives a reweighting factor $C[U]$. In this reweighting procedure the sign of the Pfaffian of the fermion matrix can also be included in the measurement as follows:

$$\langle A \rangle = \frac{\langle \text{signPf}[U] C[U] A[U] \rangle_g}{\langle \text{signPf}[U] C[U] \rangle_g}. \quad (2.9)$$

3. Simulation details

The algorithmic parameters of our TS-PHMC runs are summarised in Table 1. The runs are performed at a single lattice spacing corresponding to $\beta = 1.6$. The measured Sommer parameter for the lighter gluino masses is about $r_0/a \simeq 4$. By using the QCD scale as mentioned in the Introduction we obtain $a \simeq 0.125$ fm and a box-size $L \simeq 2$ fm on the $16^3 \cdot 32$ lattices and $L \simeq 3$ fm on the $24^3 \cdot 48$ lattices. Comparison of results from ensembles $C_{(a,b)}$ on the $16^3 \cdot 32$ lattice and \bar{C} on the $24^3 \cdot 48$ lattice at the same gluino mass allows the study of finite size effects.

An indication of the lightness of the gluino is given by the *adjoint pion* mass, $M_{a-\pi}$, extracted from the connected part of correlator of the pseudoscalar gluino bilinear (see below). The lightest simulated adjoint pion mass (run *D*) corresponds to $M_{a-\pi} \simeq 353(20)$ MeV in QCD units.

Compared with the previously used TSMB algorithm, TS-PHMC displays a substantially improved update efficiency with shorter plaquette autocorrelation times τ^{plaq} . This is particularly true in the light gluino regime where the efficiency of TSMB undergoes a strong depletion.

Some runs required the computation of the correction factor and the determination of the Pfaffian sign. We computed the correction factors for all runs in Table 1 with the exception of runs *A*, *B*, *A_s* and *B_s*. Most signs of the Pfaffian are positive; the run with largest number of negative Pfaffians is run *D* where we found 15 configurations out of 5160 with negative sign. In most cases the effect of the correction factor turned out to be negligible. This was not the case in run *D* where the effect of $C[U]$ was important for the masses of adjoint meson bound states and the gluino-glueballs. All quoted statistical errors of the measured quantities were estimated by the Γ -method [11].

4. Bound states

The bound states masses are computed from the zero-momentum correlation function of the corresponding interpolating operator \mathcal{O} .

i) Adjoint mesons. Low-energy theories [6, 7] predict a Wess-Zumino supermultiplet containing colourless composite states of two gluinos. Such states have spin-parity quantum numbers 0^- and 0^+ . In analogy to flavour singlet QCD we denote the former $a-\eta'$ and the latter $a-f_0$. To project these states on the lattice we used the gluino bilinear operators $\mathcal{O} = \bar{\lambda}\Gamma\lambda$ where $\Gamma = \gamma_5, 1$

Table 1: TS-PHMC runs algorithmic parameters with tISym at $\beta = 1.6$. Runs labelled with s have been performed with Stout-links; $\delta\tau$ refers to the total trajectory length and A_{NC} is the noisy correction acceptance.

Run	$L^3 \cdot T$	κ	# Traj.	$\delta\tau$	A_{NC} %	τ^{plaq}	ε	λ	n_1	n_2
A	$16^3 \cdot 32$	0.1800	2500	1.05	95.6	7.5	$4.25 \cdot 10^{-3}$	3.4	50	100
B	$16^3 \cdot 32$	0.1900	2700	1.05	96.4	3.08	$9.5 \cdot 10^{-4}$	3.8	80	300
Ca	$16^3 \cdot 32$	0.2000	1973	0.99	82.9	4.91	$5.0 \cdot 10^{-5}$	4.0	200	700
Cb	$16^3 \cdot 32$	0.2000	8874	0.99	88.3	27.6	$5.0 \cdot 10^{-5}$	4.0	200	700
D	$16^3 \cdot 32$	0.2020	6947	0.56	88.5	45.7	$1.0 \cdot 10^{-6}$	4.0	800	2700
\bar{A}	$24^3 \cdot 48$	0.1980	1480	0.9	89.6	4.64	$1.0 \cdot 10^{-4}$	4.0	200	600
\bar{B}	$24^3 \cdot 48$	0.1990	1400	0.9	88.7	2.65	$4.0 \cdot 10^{-5}$	4.0	270	800
\bar{C}	$24^3 \cdot 48$	0.2000	6465	1.0	88.6	7.4	$2.0 \cdot 10^{-5}$	4.0	350	1000
A_s	$24^3 \cdot 48$	0.1500	370	1.0	97.3	3.5	$5.5 \cdot 10^{-5}$	2.2	200	600
B_s	$24^3 \cdot 48$	0.1550	1730	1.0	95.6	8.04	$5.5 \cdot 10^{-5}$	2.2	200	600
C_s	$24^3 \cdot 48$	0.1570	2110	1.0	92.4	7.2	$5.5 \cdot 10^{-6}$	2.2	400	1200

respectively. The resulting gluinoball propagator consists of connected and disconnected contributions:

$$C_\Gamma(t) = \frac{1}{V_s} \sum_{\vec{x}, \vec{y}} \left\langle \underbrace{\text{Tr}_{sc}[\Gamma Q_{xx}^{-1}] \text{Tr}_{sc}[\Gamma Q_{yy}^{-1}]}_{\text{disconnected}} - 2 \underbrace{\text{Tr}_{sc}[\Gamma Q_{xy}^{-1} \Gamma Q_{yx}^{-1}]}_{\text{connected}} \right\rangle - \frac{1}{V_s} \left\langle \frac{1}{T} \sum_t \sum_{\vec{x}} \text{Tr}_{sc}[\Gamma Q_{xx}^{-1}] \right\rangle^2. \quad (4.1)$$

The connected term can be used to extract the adjoint pion mass $M_{a-\pi}$ (the last term in Eq. (4.1) vanishes for $\Gamma = \gamma_s$). OZI arguments [4] suggest $M_{a-\pi}^2 \propto m_{\tilde{g}}$ for light gluinos.

The disconnected propagators were computed by using the Stochastic Estimators Technique (SET) in the spin dilution variant to reduce the large variance. As it is the case in QCD, the disconnected diagrams are intrinsically noisier than the connected ones and dominate the level of noise in the total correlator. We performed tests on few configurations with up to $N = 40$ noisy estimators in order to study the limit at which only the gauge noise dominates the statistical error of the disconnected correlator. The optimal number of estimators was finally fixed between 16 and 22 estimates for all runs. In the case of $a-\eta'$ reasonable signal-to-noise ratio is obtained allowing the extraction of the mass from the mass fit. This was not possible for the $a-f_0$; the latter has a nonzero overlap with the vacuum, and hence its correlator has a non-vanishing vacuum contribution (the last term in Eq. (4.1)). This results in a much worse signal-to-noise ratio, and the effective mass could only be extracted at very short time separations. In the future we shall consider new variance reduction techniques for a more precise computation of the disconnected diagrams.

ii) Gluino-gluoballs. The gluino-gluoballs (\tilde{g} - g) are spin- $\frac{1}{2}$ colour singlet states of a gluon and a gluino. They are supposed to complete the Wess-Zumino supermultiplet of the adjoint mesons [6]. The full correlator is built up from plaquettes connected by a gluino propagator line:

$$C_{\tilde{g}-g}^{\alpha\beta}(\Delta t) = -\frac{1}{4} \sum_{\vec{x}, \vec{y}} \sum_{i,j,k,l} \left\langle \sigma_{ij}^{\alpha\alpha'} \text{Tr}[U_{ij}(x) \sigma^a] Q_{xa\alpha',yb\beta'}^{-1} \text{Tr}[U_{kl}(y) \sigma^b] \sigma_{kl}^{\beta'\beta} \right\rangle. \quad (4.2)$$

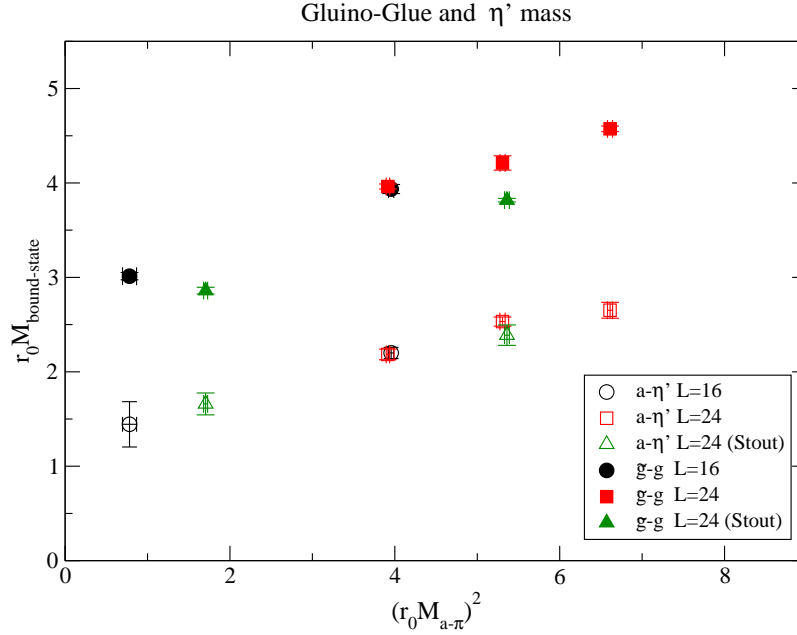


Figure 1: The masses of the low lying bound states of the $\mathcal{N} = 1$ SU(2) SYM theory. Shown are the masses multiplied by r_0 as a function the squared adjoint pion mass.

The above correlator is a matrix with two independent components in Dirac space:

$$C_{\tilde{g}-g}^{\alpha\beta}(\Delta t) = C_1(\Delta t)\delta^{\alpha\beta} + C_{\gamma_4}(\Delta t)\gamma_4^{\alpha\beta}. \quad (4.3)$$

We see agreement in the masses extracted from each component, and we choose the time antisymmetric component C_1 to fit the masses. We apply APE smearing for the links and Jacobi smearing for the fermion fields in order to optimise the signal-to-noise ratio and to obtain an earlier plateau in the effective mass.

iii) Glueballs. According to [7], 0^\pm glueballs are expected to be members of a second Wess-Zumino supermultiplet. Their study in SYM presents difficulties which closely resemble those encountered in glueball spectroscopy in QCD and, fortunately, can be overcome with the same type of techniques, namely, APE smearing with the variational method. Also in this case we use the simplest interpolating operator for the scalar glueball 0^{++} built from single space-like plaquette.

It turns out, however, that the present statistics is not enough to obtain a reliable determination of the glueball masses. Therefore, we are planning to increase the statistics.

Results. The masses of the $a-\eta'$ and the gluino-glueball are displayed in Fig. 1 as a function of the squared adjoint pion mass in units of the Sommer scale parameter. Both bound state masses appear to be characterized by a linear dependence on $(r_0 M_\pi)^2$. The gluino-glueball turns out to be appreciably heavier (50%) than the $a-\eta'$. Runs with and without Stout-smearing give consistent results for the $a-\eta'$ mass, while a discrepancy is observed for the gluino-glueball, which can be interpreted as an $O(a)$ discretisation effect. The comparison of the two runs at $(r_0 M_\pi)^2 \simeq 4$ in $(2\text{fm})^3$ and $(3\text{fm})^3$ volumes reveals small finite volume effects. The linear extrapolation of the $a-\eta'$ mass to massless adjoint pion (including the four lightest points) gives: $r_0 M_{a-\eta'} =$

1.247(48) [499(20) MeV]. A rough estimate for the gluino-gluon gives $r_0 M_{\tilde{g}-g} = 2.5 - 3$ [1000 – 1200 MeV].

5. Summary and conclusions

New results on the spectrum of bound states have been obtained by means of the TS-PHMC algorithm with noisy correction. The new algorithm, with an improved gauge action and Stout-smearred links, allows to obtain a significantly better performance compared to the previously used TSMB algorithm. This allows us to simulate in significantly larger volumes of $(2\text{ fm})^3$ and $(3\text{ fm})^3$. Our first results for the masses are within errors equal in these two cases implying that these volumes are large enough for the study of the particle spectrum. We shall systematically investigate the finite volume effects in future publications.

According to the low-energy effective theory of [6] the $a-\eta'$ and the gluino-gluon belong to the same supermultiplet and therefore should be degenerate in the SUSY limit. However our preliminary results show a gluino-gluon mass systematically heavier than the $a-\eta'$ until the lightest simulated gluino mass in the weakly broken SUSY region. Whether this outcome is a discretisation artifact or a physical effect will become clear in future studies at finer lattice spacings. If the latter case applies, the interpolating gluino-gluon operator could have dominant overlap with a member of a higher supermultiplet. The complete identification of possible supermultiplets requires the inclusion of the masses of the gluons and the scalar $a-f_0$ bound states.

The computations were carried out on Blue Gene L/P and JuMP systems at JSC Jülich, Opteron PC-cluster at RWTH Aachen and the ZIV PC-cluster of the university of Münster (Germany).

References

- [1] F. Farchioni, G. Münster, T. Sudmann, J. Wuilloud, I. Montvay and E. E. Scholz, PoS(LATTICE 2008)128.
- [2] I. Montvay, Int. J. Mod. Phys. A **17** (2002) 2377.
- [3] F. Farchioni and R. Peetz, Eur. Phys. J. C **39** (2005) 87.
- [4] G. Curci and G. Veneziano, Nucl. Phys. B **292** (1987) 555.
- [5] F. Farchioni *et al.* [DESY-Münster-Roma Collaboration], Eur. Phys. J. C **23** (2002) 719.
- [6] G. Veneziano and S. Yankielowicz, Phys. Lett. B **113** (1982) 231.
- [7] G.R. Farrar, G. Gabadadze and M. Schwetz, Phys. Rev. D **58** (1998) 015009.
- [8] C. Morningstar and M.J. Peardon, Phys. Rev. D **69** (2004) 054501.
- [9] I. Montvay and E.E. Scholz, Phys. Lett. B **623** (2005) 73.
- [10] I. Montvay, Nucl. Phys. B **466** (1996) 259.
- [11] U. Wolff, Comput. Phys. Commun. **156** (2004) 143; Erratum-ibid. **176** (2007) 383.
- [12] I. Campos *et al.* [DESY-Münster Collaboration], Eur. Phys. J. C **11** (1999) 507.